The Wip1 Phosphatase PPM1D Dephosphorylates SQ/TQ Motifs in Checkpoint Substrates Phosphorylated by PI3K-like Kinases†

Hiroshi Yamaguchi,‡ Stewart R. Durell,‡ Deb K. Chatterjee,§ Carl W. Anderson,|| and Ettore Appella*,‡

Laboratory of Cell Biology, National Cancer Institute, National Institutes of Health, Bethesda, Maryland 20892, Protein Expression Laboratory, SAIC-Frederick, Inc., National Cancer Institute at Frederick, Frederick, Maryland 21702, and Biology Department, Brookhaven National Laboratory, Upton, New York 11973

Received June 4, 2007; Revised Manuscript Received August 21, 2007

ABSTRACT: The wild-type p53-induced phosphatase Wip1 (PP2Cδ or PPM1D) is a member of the protein phosphatase 2C (PP2C) family and controls cell cycle checkpoints in response to DNA damage. p38 MAPK and ATM were identified as physiological substrates of Wip1, and we previously reported a substrate motif that was defined using variants of the p38(180pT 182pY) diphosphorylated peptide, TDDEMpT-GpYVAT. However, the substrate recognition motifs for Wip1 have not been fully defined as the sequences surrounding the targeted residues in ATM and p38 MAPK appear to be unrelated. Using a recombinant human Wip1 catalytic domain (rWip1), in this study we measured the kinetic parameters for variants of the ATM(1981pS) phosphopeptide, AFEEGpSQSTTI. We found that rWip1 dephosphorylates phosphoserine and phosphothreonine in the p(S/T)Q motif, which is an essential requirement for substrate recognition. In addition, acidic, hydrophobic, or aromatic amino acids surrounding the p(S/T)Q sequence have a positive influence, while basic amino acids have a negative influence on substrate dephosphorylation. The kinetic constants allow discrimination between true substrates and nonsubstrates of Wip1, and we identified several new putative substrates that include HDM2, SMC1A, ATR, and Wip1 itself. A three-dimensional molecular model of Wip1 with a bound substrate peptide and site-directed mutagenesis analyses suggested that the important residues for ATM(1981pS) substrate recognition are similar but not identical to those for the p38(180pT 182pY) substrate. Results from this study should be useful for predicting new physiological substrates that may be regulated by Wip1 and for developing selective anticancer drugs.

The wild-type p53-induced phosphatase Wip1[1] (PP2Cδ or PPM1D) is a member of the serine/threonine protein phosphatase 2C (PP2C) family, and its transcription is induced by the p53 tumor suppressor after exposure of cells to DNA damage-inducing agents such as ionizing radiation or UV light (*1*, *2*). The Wip1 protein is overexpressed and the *PPM1D* gene is amplified in several human cancers such as breast cancer, neuroblastoma, and ovarian clear cell adenocarcinoma (*3*−*6*). In addition, the *PPM1D* gene complements the oncogenes *Ras*, *Myc*, and *Neu* for cellular transformation of primary mouse embryo fibroblasts (*3*, *4*), indicating that Wip1 can function as an oncogene in several cancers. Disruption of *PPM1D* activates p53, $p16^{INK4a}$-$p19^{ARF}$, and/or the ataxia telangiectasia mutated (ATM) pathways and suppresses tumorigenesis in several murine models (*7*, *8*), suggesting that inhibition of Wip1's enzymatic activity or *PPM1D* gene expression may be an effective strategy for treating certain types of cancer.

The p38 mitogen-activated protein kinase (MAPK), which following DNA damage mediates the activation of p53, and a nuclear isoform of uracil DNA glycosylase (UNG2), which catalyzes base excision repair, were initially found to be physiological substrates of Wip1 (*2*, *9*). Wip1 directly interacts with both p38 MAPK and UNG2 and inactivates them through dephosphorylation of phosphothreonine present in the pTXpY amino acid sequence. Studies of enzyme kinetics of p38 MAPK and UNG2 phosphopeptides containing the site dephosphorylated by Wip1 demonstrated that the catalytic domain of Wip1 prefers diphosphorylated peptides rather than monophosphorylated peptides and that the substrate motif is X_{-1}-pT-X_{+1}-pY-X_{+3}, where X_{-1}, X_{+1}, and X_{+3} denote any amino acid, any hydrophobic amino acid, and any amino acid except Pro, respectively (*10*). In addition, the X residue in the pTXpY sequence affects the affinity for the substrate (*10*). Subsequently, a more thorough

† The research of H.Y., S.R.D., and E.A. was supported by the Intramural Research Program of the National Institutes of Health, National Cancer Institute. The research of D.K.C. was supported in part with federal funds from the National Cancer Institute, National Institutes of Health, under Contract No. N01-CO-12400. C.W.A. was supported in part at the Brookhaven National Laboratory by the Low Dose Radiation Research Program of the Office of Biological and Environmental Research of the U.S. Department of Energy.

* To whom correspondence should be addressed. Phone: (301) 402-4177. Fax: (301) 496-7220. E-mail: appellae@pop.nci.nih.gov.

‡ National Institutes of Health.

§ National Cancer Institute at Frederick.

|| Brookhaven National Laboratory.

[1] Abbreviations: ATM, ataxia telangiectasia mutated; ATR, ATM/Rad3-related; EGTA, ethylene glycol bis(β-aminoethyl ether)-*N*,*N*,*N*′,*N*′-tetraacedic acid; F_2Pab, L-2-amino-4-phosphono-4,4-difluorobutanoic acid; Fmoc, 9-fluorenylmethoxycarbonyl; IC_{50}, half maximal inhibitory concentration; MAPK, mitogen-activated protein kinase; MKK, mitogen-activated kinase kinase; NMR, nuclear magnetic resonance; PIKK, phosphatidylinositol 3-kinase-related protein kinase; PP2C, protein phosphatase 2C; pX, phosphorylated amino acid; UNG2, nuclear isoform of uracil DNA glycosylase; Wip1, wild-type p53-induced phosphatase.

10.1021/bi701096s CCC: $37.00
Published on Web 10/16/2007

understanding was obtained from the effort to develop a peptide inhibitor (*11*). Interestingly, replacing phosphothreonine by phosphoserine results in a peptide whose activity is also influenced by the intervening residue, but with a different residue-type dependency. For example, while in the wild-type p38 MAPK and UNG2, pT(G/L)pY-containing peptides are potent substrates, a pSGpY-containing analogue is inactive. However, substitution of glutamine for glycine in the latter sequence, i.e., pSQpY, resurrects activity comparable to that of the wild-type, pTGpY-containing peptides. Although not dephosphorylated, the inactive versions of the phosphoserine-containing peptides appear to still bind in the catalytice site of Wip1 since they act as competitive inhibitors. Unlike the pTXpY motif, which prefers a hydrophobic residue at the intervening position, sequences containing pS(I/V)pY were found to be the most potent inhibitors. Finally, these results are consistent with the findings that the MKK1, MKK4, and MKK6 MAPK kinases, which are activated through phosphorylation of the SXXX(S/T) motif, or JNK1 and ERK2 MAPKs, which are activated through phosphorylation of the T(P/E)Y sequence, are not physiological substrates of Wip1, in contrast to a previous report (*2*).

Analyses of *PPM1D* null mice showed defects in reproductive organs, immune function, and cell cycle control (*12*), indicating that Wip1 may have several other physiological targets and regulates important biological functions in response to DNA damage. In fact, recent studies have reported that Wip1 also dephosphorylates phosphoserine in the pSQ sequences of p53 Ser15 (*13*), Chk1 Ser345 (*13*), and ATM Ser1981 (*14*) and phosphothreonine in the pTQ sequence of Chk2 Thr68 (*15*, *16*). These substrates confirm genetic studies indicating that Wip1 may control cell cycle checkpoints in response to DNA damage. The p(S/T)Q motif is quite different from the pTXpY sequence found in p38 MAPK and UNG2, suggesting that a different consensus substrate motif for Wip1 may be utilized. Because the multiple functions of Wip1 have not been fully elucidated, identification of the physiological substrates and development of selective inhibitors should provide insight into the mechanisms that regulate multiple pathways of cell growth. In this study, we characterized a second common Wip1 substrate motif using its recombinant catalytic domain (residues 1−420 in human) and a series of ATM(1981pS)-based phosphopeptides. Several new putative substrates were identified, and new peptide inhibitors of Wip1 were synthesized on the basis of the substrate specificity defined in this study.

EXPERIMENTAL PROCEDURES

Protein Expression and Purification. The N-terminal histidine-tagged, catalytic domain of human Wip1 (residues 1−420), rWip1, and the K238D and R110E mutants were expressed in *Escherichia coli* BL21 (DE3) and purified as reported (*10*). PP2Cα was purchased from Calbiochem (La Jolla, CA).

A plasmid, pET23, containing the Wip1 catalytic domain was used for construction of the mutant D264A using the QuickChange protocol as described by the manufacturer (Stratagene, La Jolla, CA). The sequences of the oligonucleotides used for D264A were as follows: 5′-AGAAGGAGCACAGTTATTGCGCAGATTCCTTTTCTGGCAGTAG-3′ and 5′-CTACTGCCAGAAAAGGAATCTGCGCAATAACTGTGCTCCTTCT-3′. An *Fsp*I restriction enzyme site was created in the oligonucleotides (underlined) for easy screening of mutant clones. Following PCR, the product was digested with *Dpn*I to eliminate the parental plasmid. Finally, 1 μL of *Dpn*I-digested product was used for transformation into 20 μL of DH5α. Colonies were selected on ampicillin-containing plates (100 μg/mL), and mutants were screened for the presence of *Fsp*I restriction sites. Plasmids containing the designed *Fsp*I site were sequenced to confirm the mutation.

Mutant plasmid (D264A) was cotransformed with pACYC-Duet (Novagen, Madison, WI) expressing Skp and DsbC (unpublished) proteins into BL21-star competent cells (Invitrogen, Carlsbad, CA). Transformed colonies were selected on ampicillin (100 μg/mL) and chloramphenicol (15 μg/mL) containing plates. Cells were grown (800 mL) to mid-log phase in Circle Grow (Q-Biogen, Irvine, CA) at 37 °C before transfer to a 16 °C incubator. After incubation for approximately 15 min, cells were induced with 0.75 mM isopropyl 1-thio-β-D-galactopyranoside for 16 h. Cells were harvested and used for purification as described previously (*10*).

Peptide Synthesis. Peptides were synthesized by the solid-phase method with 9-fluorenylmethoxycarbonyl (Fmoc) chemistry as described previously (*10*). To estimate peptide concentrations by spectrometry, a Gly-Tyr sequence was introduced at the C-terminus of peptides that did not contain aromatic amino acids (Tyr or Trp) in their sequence. L-2-Amino-4-phosphono-4,4-difluorobutanoic acid (F_2Pab) was coupled as Fmoc-F_2Pab-OH (AnaSpec Inc., San Jose, CA). Cyclic peptides were synthesized as described previously (*11*). The purity of the peptides was determined to be >95% by analytical reversed-phase high-performance liquid chromatography. The masses of peptides were confirmed by matrix-assisted laser desorption ionization time-of-flight mass spectrometry (Micromass, Beverly, MA).

Phosphatase Assay. Phosphatase activity was measured by a malachite green/molybdate-based assay as described previously (*10*). Reactions were carried out in 50 mM Tris−HCl, pH 7.5, 0.1 mM EGTA, 0.02% 2-mercaptoethanol, and 30 mM $MgCl_2$ for 7 min at 30 °C. The amount of phosphate released was calculated using a phosphate standard curve. To determine the kinetic parameters K_m and k_{cat}, the initial velocities (v) were measured at various concentrations of substrate peptide ([S]), and data were fitted to the Michaelis−Menten equation (eq 1).

$$v = k_{cat}[S]/(K_m + [S]) \quad (1)$$

The IC_{50} values for inhibition of phosphatase activity by the phosphopeptide inhibitors were measured using 30 μM ATM(1981pS) substrate peptide in 50 mM Tris−HCl, pH 7.5, 0.1 mM EGTA, 0.02% 2-mercaptoethanol, 40 mM NaCl, and 30 mM $MgCl_2$ for 7 min at 30 °C. The phosphatase and phosphopeptide inhibitors were preequilibrated at 30 °C for 6 min. The inhibition percentages were estimated by eq 2,

$$\text{inhibition (\%)} = 100[1 - (A - A_0)/(A_{100} - A_0)] \quad (2)$$

where A and A_{100} are absorbance intensities at 630 nm with and without the peptide inhibitor, respectively, and A_0 is the absorbance of the sample without phosphatase. The IC_{50} values were estimated by a sigmoidal dose−response equation. The apparent inhibitory constant K_i values were estimated using eq 3 (*17*), where [S] is the concentration of the substrate peptide and K_m is the Michaelis constant.

$$K_i = IC_{50}/(1 + [S]/K_m) \quad (3)$$

Molecular Modeling and Computational Docking. Atomic-scale, computer modeling of the interaction of ATM(1981pS) and Wip1 was performed in a manner analogous to that of our previous studies (*10*, *11*). The three-dimensional model of the catalytic site of Wip1 was the same as previously described, which was developed from the crystal structure of human PP2Cα (*18*). The three-dimensional model of the ATM(1981pS) peptide (AFEEGpSQSTTI) was created and energy minimized with the CHARMM software package (*19*). Docking of the peptide to the protein was simulated and analyzed with the interlocked Autodock3 (*20*) and AutoDockTools (*21*) software packages. While the side chains of the Wip1 structure were static, all non-amide, single-bond dihedral angles of the ATM phosphopeptide were allowed to rotate. A square search grid of 33.75 Å edge length (0.375 Å/point resolution) was used, arbitrarily centered over the active site of Wip1. Over 440 individual docking simulations were conducted, starting with randomly selected dihedral angles and positions in the grid for the ATM peptide. The Larmarckian genetic algorithm was employed, with a population size of 150 and a maximum number of generations of 1500. Default values were used for all other algorithmic parameters.

RESULTS

Determination of a New Optimal Substrate Motif of the Human Wip1 Catalytic Domain (rWip1). It was reported that Wip1 dephosphorylates ATM Ser1981 in vitro and in vivo, a site critical for ATM activation, and modulates ATM-dependent signaling pathways (*14*). To assess the effect of individual side chains surrounding the pSQ sequence, we first measured the kinetic parameters for variants of the ATM(1976−1986)(1981pS) phosphopeptide, AFEEGpSQSTTI, in which individual residues were substituted with Ala (Table 1). In this experiment, we used the catalytic domain of human Wip1 (rWip1), which has phosphatase activity comparable to that of full-length Wip1 (*10*). The largest effects were seen in the peptides with Ala or Asn substituted at position +1 for Gln (Q1982A or Q1982N); these peptides were not dephosphorylated by rWip1 (Table 1). Peptides with Ala substituted for Glu at position −3 or −2 (E1978A and E1979A) were poorer substrates for rWip1 than the wild-type peptide, while other Ala-substituted peptides, except for the S1983A peptide, showed k_{cat}/K_m similar to that of the wild-type peptide. A phosphopeptide with Ala substituted for Ser at position +2 (S1983A) showed a 1.4-fold decrease in K_m but had the same k_{cat} as the wild-type peptide. From these results, we conclude that Gln in the pSQ sequence, the acidic residues at positions −3 and −2, and the residue at position +2 in the ATM(1981pS) peptide are important for substrate recognition by rWip1.

Table 1: Kinetic Parameters for the Dephosphorylation of ATM(1976−1986)(1981pS) Analogues by rWip1 at pH 7.5 and 30 °C[a]

substrate	sequence[b]	K_m (μM)	k_{cat} (s^{-1})	k_{cat}/K_m ($\times 10^3$ M^{-1} s^{-1})
wild-type	AFEEGpSQSTTI	31 ± 2	2.9 ± 0.1	94
F1977A	A**A**EEGpSQSTTI	41 ± 5	3.0 ± 0.1	73
E1978A	AF**A**EGpSQSTTI	44 ± 1	2.4 ± 0.02	55
E1979A	AFE**A**GpSQSTTI	65 ± 4	2.5 ± 0.1	38
G1980A	AFEE**A**pSQSTTI	34 ± 4	2.6 ± 0.1	77
Q1982A	AFEEGpS**A**STTI	ND	ND	ND
S1983A	AFEEGpSQ**A**TTI	23 ± 2	3.0 ± 0.1	130
T1984A	AFEEGpSQS**A**TI	25 ± 2	2.9 ± 0.1	116
T1985A	AFEEGpSQST**A**I	26 ± 2	3.0 ± 0.1	115
I1986A	AFEEGpSQSTT**A**	28 ± 2	3.1 ± 0.1	111
Q1982N	AFEEGpS**N**STTI	ND	ND	ND
pS1981pT	AFEEG**pT**QSTTI	9 ± 2	0.8 ± 0.03	89
E1978/1979A	AF**AA**GpSQSTTI	91 ± 3	1.9 ± 0.03	21
E1978/1979D	AF**DD**GpSQSTTI	28 ± 1	2.8 ± 0.1	100
E1978/1979K	AF**KK**GpSQSTTI	ND	ND	ND
S1983V	AFEEGpSQ**V**TTI	22 ± 1	3.0 ± 0.03	136
S1983I	AFEEGpSQ**I**TTI	22 ± 1	3.1 ± 0.04	141
S1983L	AFEEGpSQ**L**TTI	21 ± 1	3.3 ± 0.1	157
S1983D	AFEEGpSQ**D**TTI	17 ± 1	2.8 ± 0.1	165
S1983E	AFEEGpSQ**E**TTI	26 ± 0.4	2.8 ± 0.01	108
S1983K	AFEEGpSQ**K**TTI	214 ± 41	3.0 ± 0.4	14
S1983P	AFEEGpSQ**P**TTI	57 ± 5	2.5 ± 0.1	44
S1983F	AFEEGpSQ**F**TTI	21 ± 2	2.7 ± 0.1	129
S1983Y	AFEEGpSQ**Y**TTI	37 ± 3	4.1 ± 0.1	111
S1983pY	AFEEGpSQ**pY**TTI	20 ± 1	3.9 ± 0.1	195

[a] Values represent averages from 3−4 independent experiments. ND = not determined due to undetectable dephosphorylation. [b] Substituted amino acids are indicated in bold.

Recently we reported that, for the case of the diphosphorylated peptides, substituting phosphoserine for phosphothreonine results in either a substrate or an inhibitor depending on the type of intervening residue. Specifically, a pSQpY-containing peptide is a good substrate, and pS(I/V)pY-containing peptides are good inhibitors (*11*). Therefore, we sought to know the effect of substituting phosphothreonine for phosphoserine in the monophosphorylated, ATM-type motif. Interestingly, the pS1981pT peptide also acted as a substrate for rWip1, with a k_{cat}/K_m similar to that of the wild-type peptide (Table 1). Thus, rWip1 also dephosphorylates phosphothreonine in the pTQ motif.

Because each of the Glu residues at positions −3 and −2 in the ATM peptide have an influence on substrate recognition by rWip1 (Table 1), we next tested doubly substituted ATM peptides at these positions (Table 1). A di-Ala-substituted peptide (E1978/1979A) had a higher K_m and lower k_{cat} compared to those of the wild-type peptide or mono-Ala-substituted peptides (E1978A or E1979A), indicating that the E1978/1979A peptide is a poor substrate. A di-Asp-substituted peptide (E1978/1979D) showed K_m and k_{cat} values similar to those of the wild-type peptide. In contrast, a di-Lys-substituted peptide (E1978/1979K) was not dephosphorylated by rWip1. These results indicate that the acidic residues at both positions −3 and −2 in the ATM peptide have a positive influence on substrate recognition through an electrostatic interaction with basic residue(s) in the catalytic site of rWip1.

To gain more information about the substrate specificity of rWip1, several substituted ATM peptides at position +2 were analyzed (Table 1). Like the Ala-substituted peptide

Table 2: Kinetic Parameters for the Dephosphorylation of p(S/T)Q-Sequence- or pT*X*pY-Sequence-Containing Phosphopeptides by rWip1 at pH 7.5 and 30 °C[a]

substrate	sequence[b]	K_m (μM)	k_{cat} (s^{-1})	k_{cat}/K_m ($\times 10^3$ M^{-1} s^{-1})
model substrate	AADDA**pS**QLAAY	22 ± 1	3.5 ± 0.1	159
p53(15pS)	VEPPL**pS**QETFS	13 ± 1	1.8 ± 0.04	138
p53(1−39)(15pS)	−VEPPL**pS**QETFS−[c]	11 ± 1	1.7 ± 0.1	155
Chk1(345pS)	QGISF**pS**QPTCPD	52 ± 4	1.3 ± 0.1	25
Chk2(68pT)	LETVS**pT**QELYS	5.3 ± 1	1.2 ± 0.02	226
H2A.X(139pS)	KATQA**pS**QEY	62 ± 6	3.0 ± 0.1	48
Rad17(645pS)	SELPA**pS**QPQPF	85 ± 14	1.6 ± 0.2	19
Nbs1(343pS)	PGPSL**pS**QGVSV	401 ± 174	2.1 ± 0.7	5
HDM2(395pS)	ESEDY**pS**QPSTS	23 ± 1	1.4 ± 0.02	61
SMC1A(957pS)	QEEGS**pS**QGEDS	27 ± 1	2.7 ± 0.1	100
ATR(1876pS)	SPGDS**pS**QEDSL	20 ± 2	3.9 ± 0.1	195
Wip1(25pT)	YMEDV**pT**QIVVE	5.4 ± 1.3	0.4 ± 0.01	74
Wip1(46pS)	RRSL**pS**QPLPPY	ND	ND	ND
Wip1(214pT)	AVEV**pT**QDHKPY	25 ± 2	1.4 ± 0.04	56
Wip1(280pS)	GDLW**pS**YDFFS	ND	ND	ND
p38(180pT 182pY)	TDDEM**pT**G**pY**VAT	31 ± 3	2.0 ± 0.1	64
p38(180pT)	TDDEM**pT**GYVAT	84 ± 34	1.0 ± 0.2	12
p38(pTQpY)	TDDEM**pT**Q**pY**VAT	8 ± 2	0.5 ± 0.02	63

[a] Values represent averages from 3−4 independent experiments. ND = not determined due to undetectable dephosphorylation. [b] Phosphorylated amino acids are indicated in bold. [c] First 39 residues of human p53 (MEEPQSDPSVEPPL**pS**QETFSDLWKLLPENNVLSPLPSQA).

(S1983A), hydrophobic amino acid-substituted peptides (S1983V, S1983I, and S1983L) exhibited higher k_{cat}/K_m values than the wild-type peptide. Acidic amino acids (Asp and Glu), aromatic amino acids (Phe and Tyr), or phosphotyrosine-substituted peptides also showed enhancement of the k_{cat}/K_m values. In contrast, k_{cat}/K_m values for Lys- and Pro-substituted peptides decreased by 6.7- and 2.1-fold, respectively. The Lys-substituted peptide exhibited an especially significant increase of K_m, although the k_{cat} for this peptide was very similar to that of other substituted peptides. These data indicated that the substitution at position +2 affects the substrate's affinity for rWip1, as judged by the K_m values.

From the ATM(1981pS) peptide substitution analysis, we were able to define the motif (D/E)-(D/E)-X_{-1}-p(S/T)-Q-X_{+2} as important for substrate recognition by rWip1, where X_{-1} and X_{+2} denote any amino acid and any amino acid except basic amino acids and Pro, respectively. On the basis of the above results, we synthesized a model peptide, AA**DD**A**pSQL**AAY, and measured its kinetic parameters. As expected, this peptide was a good substrate for rWip1 (Table 2) and exhibited a k_{cat}/K_m similar to that of the ATM peptide, AF**EE**G**pSQL**TTI, as seen in Table 1.

Several proteins have been identified that appear to be substrates of Wip1. Therefore, we analyzed the kinetic parameters for p(S/T)Q peptides that contained the sequences of reported physiological substrates such as p53 Ser15, Chk1 Ser345, and Chk2 Thr68 (*13*, *15*, *16*) and nonsubstrates, H2A.X Ser139, Rad17 Ser645, and Nbs1 Ser343 (*14*). The p53(15pS) and Chk2(68pT) peptides having acidic residues before and after their p(S/T)Q sequences were dephosphorylated by rWip1 and showed higher k_{cat}/K_m values than the ATM(1981pS) peptide (Table 2). The result for the p53-(15pS) peptide also revealed that a Pro residue before the pSQ sequence does not affect substrate dephosphorylation. Moreover, a longer chain length of p53(1−39)(15pS) compared to p53(10−20)(15pS) did not influence substrate recognition (Table 2), indicating that rWip1 recognizes a narrow region around the pSQ sequence. In contrast, the H2A.X(139pS), Rad17(645pS), and Nbs1(343pS) peptides were poor substrates for rWip1 because these peptides have only one or completely lack acidic residues surrounding their pSQ sequences. These results show that the new substrate specificity can identify known physiological substrates of Wip1. Although Chk1 Ser345 has been reported as a physiological substrate for Wip1 (*13*), because it has no acidic residues surrounding Ser345, the Chk1(345pS) peptide was found to be a poor substrate compared to the ATM-(1981pS), p53(15pS), and Chk2(68pT) peptides. From these results, we can define X_{-4}-X_{-3}-X_{-2}-X_{-1}-p(S/T)Q-X_{+2}-X_{+3} as the new substrate motif of rWip1, where for X_{-4}, X_{-3}, and X_{-2} acidic amino acids are preferred. The X_{+2} position can be occupied by any amino acid except basic amino acids or Pro, whereas the X_{-1} and X_{+3} positions can accept any amino acid.

Identification of Putative Substrates of rWip1. Because the ATM and ATM/Rad3-related (ATR) kinases phosphorylate physiological substrates of Wip1, we used the SCANSITE genomic search program (*22*) to find potential additional putative substrates; among these potential new targets were MDM2, SMC1A, ATR, and Wip1 itself, each of which is involved in cell cycle regulation. Human MDM2 (HDM2) is an E3 ligase that controls p53 function through its degradation (*23*). SMC1A is involved in chromosome cohesion during the cell cycle and in DNA repair (*24*). ATR, like ATM, is a member of the phosphatidylinositol 3-kinase-related protein kinase (PIKK) family and regulates cell cycle checkpoints in response to DNA damage (*25*). We then evaluated the ability of rWip1 to dephosphorylate the p(S/T)Q substrate peptide sequences from these potential substrates.

The residues of HDM2, Ser395, and SMC1A, Ser957, are known as ATM or ATR phosphorylation sites, and these phosphorylations are important for regulating cell cycle checkpoints and DNA repair in response to DNA damage (*25*). As shown in Table 2, both the HDM2(395pS) and SMC1A(957pS) peptides, which have acidic residues before and/or after their pSQ sequences, were better substrates for rWip1 than nonsubstrate peptides such as H2A.X(pS139), Rad(pS645), or Nbs1(pS343). Because the HDM2(395pS)

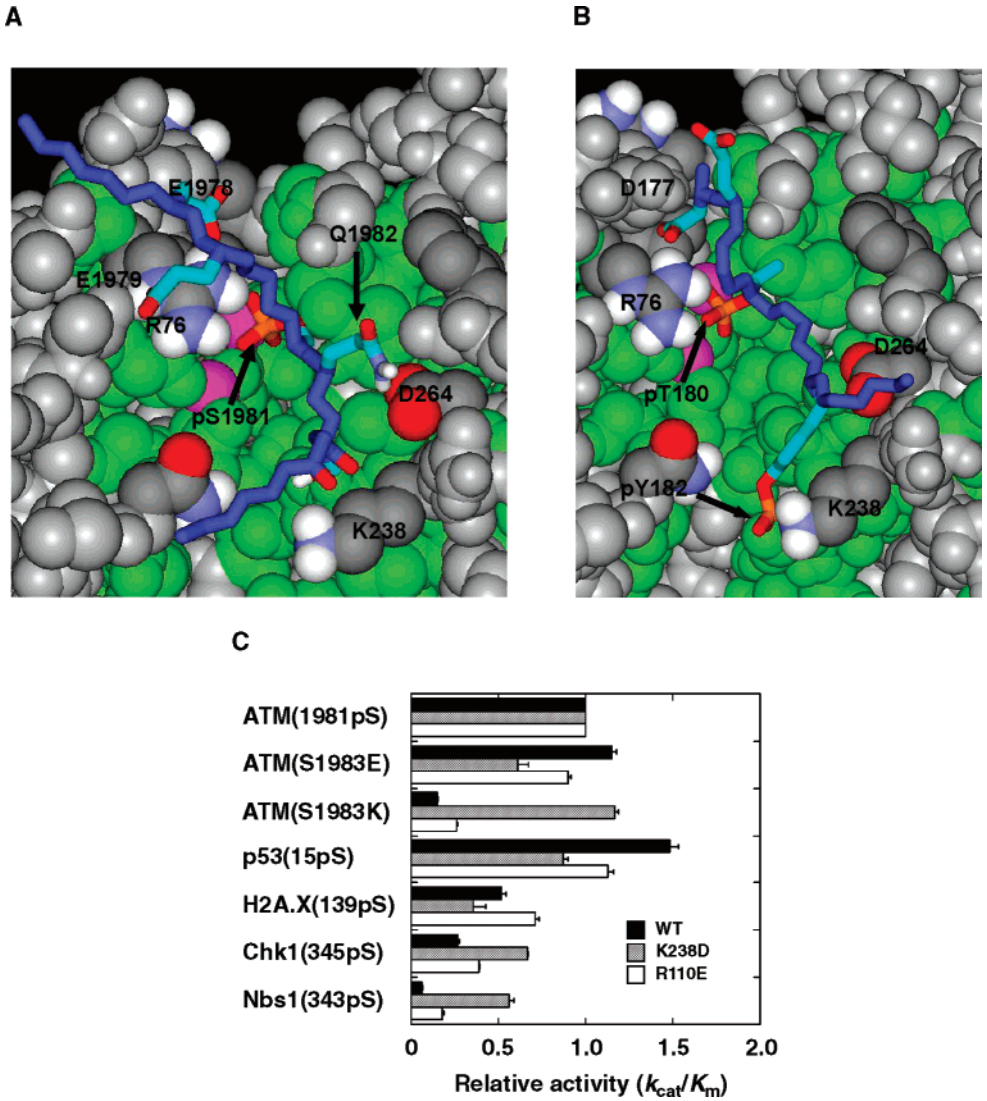

FIGURE 1: Substrate recognition of Wip1. Molecular model from docking simulations of Wip1 complexed with the ATM(1981pS) peptide (AFEEGpSQSTTI) (A) and the p38(180pT 182pY) peptide (DEMpTGpYVA) (B). Residues outside the active site are gray. The two magnesium ions are colored magenta. (C) Substrate preference of the K238D (hatched box) and R110E (open box) mutants. The results are presented as k_{cat}/K_m relative to that of the ATM(1981pS) wild-type (filled box) substrate peptide. The graph shows the mean ± standard error for at least three experiments. All assays were performed at 30 °C and pH 7.5.

peptide has Pro at position +2, the k_{cat}/K_m is lower than that of the ATM(1981pS) peptide, but it was similar to that of the p38(180pT 182pY) peptide. The search program also identified ATR Ser1876 as a potential site of phosphorylation by the PIKK family members. This site was previously unknown; interestingly, the sequence surrounding Ser1876 has acidic residues without any basic residues. As expected, the ATR(1876pS) peptide was rapidly dephosphorylated by rWip1 (Table 2). We also found that the Wip1(25pT) and Wip1(214pT) peptides but not the Wip1(46pS) and Wip1-(280pS) peptides were substrates, although neither Thr25 nor Thr214 has been identified as an in vivo phosphorylation site.

p(S/T)Q Substrate Recognition by Wip1. Computer docking simulation studies were conducted to identify the energetically favorable interactions responsible for binding of the p(S/T)Q motif-containing peptides to Wip1. The ATM-(1981pS) peptide (AFEEGpSQSTTI) was again used as the representative of this motif, since this was the subject of our kinetic studies of systematic mutations (Table 1), which provided data on the influences of the adjacent residues. The simulations resulted in 440 structures with docking energies ranging from −19.9 to −2.0 kcal/mol. Sorting these into 10 equally spaced bins spanning the energy range (i.e., the frequency distribution of energies) resulted in four structures in the lowest energy category. For all of these, the phosphate group of the 1981pS residue was located in the position of the catalytic site analogous to that of the free PO_4^{3-} group in the PP2Cα crystal structure (*18*), as required for phosphatase activity (*26*). This is likely due to the strong electrostatic interaction between the phosphate group (−2e) of the peptide and the dual-Mg^{2+}−ligand complex and conserved R76 residue (1e) (R33 in PP2Cα) core of the catalytic site (*18*). Of these four, two of the lowest energy conformations shared the additional feature of the peptide Q1982 residue forming a stabilizing, hydrogen bond interaction with the D264 residue of Wip1. This is demonstrated in Figure 1A, which for clarity illustrates only one of these two peptides. All four of the lowest energy peptides have additional, stabilizing interactions at both the N- and C-terminals. However, these differ for each due to conformational variation at the ends. For the structure in the figure,

these extra interactions include salt bridges/hydrogen bonds between the peptide E1978 and E1979 residues and the conserved R76 residue of Wip1, a hydrogen bond between the peptide S1983 and the conserved K218 and/or K238 of Wip1, and a hydrogen bond with the backbone carbonyl oxygen and/or side chain of the peptide T1984 and the K238 of Wip1. Three of the four lowest energy peptides share the orientation shown in Figure 1A, with the N-terminus on the top and the C-terminus on the bottom. As seen in Figure 1B, this mode of binding is very similar to that predicted for the diphosphorylated p38(180pT 182pY) peptide (*10*). However, the remaining ATM(1981pS) peptide had the reverse orientation, with the N-terminus on the bottom. In this case, the negatively charged E1978 and E1979 peptide residues interacted with the positively charged K238 and K218 residues of Wip1, respectively (not shown).

Roles of Lysine 238 and Aspartic Acid 264 for p(S/T)Q Substrate Recognition. To better define the roles of residues K238 and D264 in p(S/T)Q substrate recognition, the kinetic parameters for rWip1 single amino acid mutants were measured. K238 was changed to Asp, as was done previously (*10*), and D264 was changed to Ala. We also tested the R110 mutant (R110E), which could potentially interact with the negatively charged, acidic residues at the N-terminus of the peptide. However, similar to the p38(180pT 182pY) peptide (*10*), rWip1(R110E) showed a similar p(S/T)Q substrate preference compared to wild-type rWip1 (Figure 1C) (see the Suporting Information for the full list of kinetics parameters of the rWip1 mutants). In contrast, the H2A.X-(139pS) peptide was a slightly better substrate for the R110E mutant than for wild-type rWip1, suggesting that Lys at position −5 in the H2A.X(139pS) sequence may interact with the Glu in mutant rWip1(R110E). These results support the binding orientation shown in Figure 1A, where the E1978 and E1979 residues in the ATM sequence (at motif positions −3 and −2) are too far to interact with R110, but the Lys residue in the H2A.X(139pS) sequence (at motif position −5) is too far from the active site to be able to make a physical contact.

rWip1(K238D) showed decreased k_{cat}/K_m values for the p53(15pS) and ATM(S1983E) peptides, which have Glu at position +2, compared with that of the wild-type ATM-(1981pS) peptide, which has Ser at that position (Figure 1C). In contrast, the ATM(S1983K) peptide, having Lys at position +2, was a better substrate for rWip1(K238D). The K_m for the ATM(S1983K) peptide (22 ± 1 μM) is 10-fold lower than that with wild-type rWip1 (214 ± 41 μM in Table 1), while the k_{cat} values with the K238D mutant and wild type are similar: 3.6 ± 0.1 and 3.0 ± 0.4 s^{-1}, respectively. As for wild-type rWip1, the H2A.X(139pS), Chk1(345pS), and Nbs1(343pS) peptides, which do not contain charged residues surrounding their pSQ sequences, were poor substrates for rWip1(K238D). These results indicate that K238 interacts with the residue at position +2 in the p(S/T)Q peptides, as suggested by the docking model.

Because K238 interacts with both the ATM(1981pS) and p38(180pT 182pY) peptides, we next remeasured the kinetic parameters for p38 peptides with wild-type rWip1 (Table 2). As shown previously (*10*), the k_{cat}/K_m for the diphosphorylated p38(180pT 182pY) peptide was 5.3-fold higher than that of the monophosphorylated p38(180pT) peptide. Likewise, the diphosphorylated ATM(S1983pY) peptide, which has a pSQpY sequence, was a better substrate than the monophosphorylated ATM(S1983Y) peptide, which has a pSQY sequence (Table 1). However, in this case the difference in k_{cat}/K_m was only 1.7-fold. This may reflect that the ATM peptide/rWip1 complex is more stabilized by the interaction of the Q at the +1 position (which was present in both mono- and diphosphorylated peptides) than the interaction of the substituted phosphotyrosine.

Table 3: Kinetic Parameters for the Dephosphorylation of Phosphopeptides by PP2Cα at pH 7.5 and 30 °C[a]

substrate	K_m (μM)	k_{cat} (s^{-1})	k_{cat}/K_m (10^3 M^{-1} s^{-1})
pThr peptide[b]	109 ± 2	5.2 ± 0.04	48
p38(180pT 182pY)	74 ± 17	2.0 ± 0.3	27
ATM(1981pS)	ND	ND	ND
p53(15pS)	ND	ND	ND
H2A.X(139pS)	ND	ND	ND
Chk1(345pS)	ND	ND	ND
Chk2(68pT)	289 ± 57	4.0 ± 0.5	14
Rad17(645pS)	ND	ND	ND
Nbs1(343pS)	ND	ND	ND
HDM2(395pS)	ND	ND	ND
SMC1A(957pS)	ND	ND	ND
ATR(1876pS)	ND	ND	ND
ATM(pS1981pT)	411 ± 138	7.8 ± 2.2	19

[a] Values represent averages from triplicate experiments. ND = not determined due to undetectable dephosphorylation. [b] RRApTVA.

We next tested the two classes of substrates with the rWip1(D264A) mutant. For the ATM(1981pS) peptide, the substitution led to a decrease in k_{cat}/K_m from 94 × 10^3 (Table 1) to 15 × 10^3 M^{-1} s^{-1}, a greater than 6-fold change. Interestingly, the p38 peptide, with the pTGpY motif, also experienced a decrease in k_{cat}/K_m: from 64 × 10^3 (Table 2) to 16 × 10^3 M^{-1} s^{-1}, a 4-fold change. That the decrease was larger for the ATM peptide indicates that the D264 residue of Wip1 plays a larger role than it does for the p38 peptide. To further examine how the binding of the ATM and p38 peptides might be related, we compared the kinetics of native (pTGpY) and mutant (pTQpY) p38 peptides with that of wild-type rWip1. As seen in Table 2, the glutamine substitution leads to an increase in the binding affinity, with an approximate 4-fold decrease in the K_m. Suprisingly, though, the k_{cat} also decreased by 4-fold, resulting in an unchanged k_{cat}/K_m value.

Comparison of rWip1 to PP2Cα with Regard to Peptide Substrate Preference. Both Wip1 and PP2Cα dephosphorylate the phosphothreonine of the pTGpY sequence from the p38 MAPK protein or its peptide in vivo and in vitro (*2*, *10*, *27*); however, kinetic studies showed that diphosphorylated peptides with the pTGpY sequence are better substrates for Wip1 than monophosphorylated peptides, while PP2Cα prefers monophosphorylated peptides with pTGY or RXpT sequences (*10*). These results indicate that the optimal substrate motif of PP2Cα differs from that of Wip1. Since, in addition to K238, PP2Cα lacks a residue analogous to the D264 in Wip1 (see the sequence alignment in ref *10*), we measured the kinetic parameters for the p(S/T)Q peptides with PP2Cα. The pThr peptide (RRApTVA) was used as a positive control substrate (*28*). As reported previously (*10*), PP2Cα dephosphorylated the p38(180pT 182pY) diphosphorylated peptide and the monophosphorylated pThr peptide (Table 3). However, all tested pSQ peptides including the ATM(1981pS) peptide and the putative substrates of rWip1

(HDM2 Ser395, SMC1A Ser957, and ATR Ser1876) were not dephosphorylated by PP2Cα. In contrast, the pTQ peptides including the ATM(pS1981pT) peptide were dephosphorylated by PP2Cα, but they were very poor substrates compared with the p38(180pT 182pY) peptide. These results suggest that the substrate preferences of PP2Cα and rWip1 are different and that PP2Cα has a preference for phosphothreonine-containing substrates.

Peptide Inhibitor Based on the p(S/T)Q Peptide. To uncover an inhibitor of Wip1 that could be generally used as a therapeutic drug, we next synthesized peptide analogues using the p(S/T)Q peptide sequence. We previously identified a selective cyclic phosphopeptide inhibitor, c(MpSIpYVAC), of the catalytic site of Wip1 based on the p38(180pT 182pY) diphosphorylated sequence (*11*). As seen by comparing parts A and B of Figure 1, the predicted binding mode of the p(S/T)Q peptide with the catalytic site of Wip1 is similar to that of the p38(180pT 182pY) peptide. Therefore, peptide inhibitors based on the p(S/T)Q substrate sequence might also work to bind the catalytic site of Wip1 and inhibit its phosphatase activity.

To test this possibility, we synthesized two phosphoserine mimetic-containing peptides, Ac-VEPPL**F_2Pab**QETFY-NH_2 and Ac-VEPPL**F_2Pab**Q**pY**TFS-NH_2, based on the p53(15pS) sequence. L-2-Amino-4-phosphono-4,4-difluorobutanoic acid (F_2Pab), which has a chemical structure similar to that of phosphoserine (*11*, *29*), was introduced as a nonhydrolyzable phosphoserine mimetic. The K_i values for inhibition of rWip1 were measured at a constant concentration of the ATM(1981pS) peptide as a substrate as described in the Experimental Procedures. To compare with the previous results, the p38 substrate-derived, cyclic peptide c(MpSIpYVAC) was found to have a K_i of 1.2 ± 0.1 μM. This is similar to the K_i value of 0.9 ± 0.1 μM obtained when the p38(180pT 182pY) peptide was used as the substrate (*11*). This suggests that both the p(S/T)Q and pTXpY motif-containing peptides are recognized by the same catalytic site of rWip1. Both F_2Pab peptides were found to inhibit the activity of rWip1, although their activities were weaker than that of c(MpSIpYVAC). The estimated K_i of 70 ± 9 μM for Ac-VEPPL**F_2Pab**Q**pY**TFS-NH_2 is neatly 50% better than the 135 ± 13 μM obtained for Ac-VEPPL**F_2Pab**QETFY-NH_2, suggesting that the phosphotyrosine in the first peptide inhibitor interacted more strongly with K238 in rWip1 than the Glu residue of the latter. This result is consistent with the kinetic results showing that the ATM(S1983pY) peptide was dephosphorylated 1.8-fold more rapidly than the ATM(S1983E) peptide (Table 1) and is possibly due to the greater negative charge of the phosphate group (−2e) compared to the Glu residue (−1e). In addition, the rWip1(K238D) mutant and PP2Cα, which also lacks a positively charged residue at the position analogous to K238 in wild-type Wip1, were not inhibited by Ac-VEPPL**F_2Pab**Q**pY**TFS-NH_2. We also analyzed the inhibitory activities of F_2Pab-containing linear peptides that do not contain negative charges at position +2, Ac-AFEEG**F_2Pab**QSTTI and Ac-AADDA**F_2Pab**QLAAY-NH_2, based on the ATM(1981pS) and model substrate sequences, respectively. As expected, these peptides showed very poor inhibitory activities (K_i > 200μM). We next synthesized a cyclic peptide, c(L**F_2Pab**Q**pY**TYC), based on the published cyclic peptide inhibitor c(MpSIpYVAC) (*11*). However, the estimated K_i of 93 ± 14 μM was slightly lower than that obtained for the Ac-VEPPL**F_2Pab**Q**pY**TFS-NH_2 linear peptide, indicating that further optimization is required to achieve the same degree of inhibition previously achieved for the c(MpSIpYVAC) peptide (*11*).

DISCUSSION

Substrates of Wip1. Identification of the physiological substrates of Wip1 is important to understand its biological mechanisms. Recent studies have reported that Wip1 dephosphorylates phosphoserine or phosphothreonine in the p(S/T)Q sequences of p53 Ser15, Chk1 Ser345, ATM Ser1981, and Chk2 Thr68 (*13*−*16*), suggesting that Wip1 may have an important role in controlling cell cycle checkpoints in response to DNA damage. Although p38 MAPK and UNG2, which both have the pTXpY sequence, were initially found to be physiological substrates (*2*, *9*), other Wip1 substrate proteins with the pTXpY sequence have not been reported. This suggests that Wip1 may dephosphorylate mainly substrates with the p(S/T)Q sequence.

It appears that the p(S/T)Q sequence is quite different from the pTXpY sequence. To characterize the substrate specificity of Wip1, we measured the kinetic parameters of the p(S/T)Q peptides that contained the sequences of reported physiological substrates or nonsubstrates. We found that Gln at position +1 in the p(S/T)Q sequence is an essential residue for substrate recognition by rWip1 (Table 1) and that acidic residues surrounding the p(S/T)Q sequence have a positive influence, while basic residues have a negative influence (Table 1). From these results, we were able to discriminate between physiological substrates and nonsubstrates of Wip1. In addition, we identified several putative substrates for Wip1 that include SMC1A Ser957, HDM2 Ser395, and ATR Ser1876. ATM phosphorylates Ser957 of SMC1A, and interference with this phosphorylation abrogates the S-phase checkpoint (*30*, *31*). ATM also phosphorylates Ser395 of HDM2 in response to DNA damage (*32*). Phosphorylated HDM2 is less capable of promoting the nucleocytoplasmic shuttling of p53 and its subsequent degradation, thereby enabling p53 accumulation (*32*). In addition to SMC1A Ser957 and HDM2 Ser395, PIKK family members such as ATM or ATR phosphorylate the sequences of p53 Ser15, Chk1 Ser345, Chk2 Thr68, and ATM Ser1981 (*25*). Moreover, an optimal substrate motif for ATM kinase activity, identified by a peptide library approach (*33*), is very similar to our rWip1 substrate motif, suggesting that Wip1 may control the biological functions of substrates of PIKK family members or PIKK members themselves which are engaged in several pathways.

The SCANSITE program indicated that ATR Ser1876 is a potential site phosphorylated by PIKK family members. The PIKK family contains a conserved C-terminal FAT domain (*34*). Like ATM Ser1981, which is a site autophosphorylated by ATM itself and dephosphorylated by Wip1 (*14*), ATR Ser1876 is also within the FAT domain. In addition, putative substrates for Wip1 may help researchers to identify additional pathways modulated by Wip1.

Substrate Recognition by Wip1. As has been commented previously (*35*), the catalytic site of the PP2C family is relatively open and exposed compared to those of other phosphatase families. This is consistent with our discovery of at least two distinct substrate motifs for Wip1. Obviously,

for the catalytic activity to occur, all substrates must bind so that the targeted phosphate group of phosphoserine or phosphothreonine is positioned near the metal/ligand core, presumably according to the mechanism described by Jackson et al. (*26*). The picture that has emerged from this and our previous studies (*10*, *11*) is that the two motifs result from divergent mechanisms for stabilizing the binding of the substrate in catalytically permissive conformations in the active site. While both the p38 MAPK and ATM-type substrate motifs employ negatively charged residues N-terminal to where the phosphorylated target resides, they differ on the C-terminal side. As we demonstrated previously (*10*), the main secondary interaction for the p38-type substrates with the pTXpY motif is between the negatively charged phosphate group of phosphotyrosine (−2e) and the K238 and K218 residues of Wip1 (1e each). These interactions originally were predicted by docking simulations and then confirmed by kinetic studies with single point mutations in both the substrate and the enzyme. In contrast, the ATM-type substrates with the p(S/T)Q motif lack a second phosphorylated residue and thus must utilize an alternative means for binding C-terminal to the phosphorylated residue. As demonstrated here, docking simulations pointed to a possible hydrogen bond interaction between the substrate's Gln at position +1 and the D264 residue of Wip1 (Figure 1A). The importance of the Gln is shown in Table 1, where the Q1982A and Q1982N point mutations in the ATM peptide both eliminated observable enzymatic activity. Of the two, the latter, conservative mutation is especially informative because the change from Gln to Asn involves only a relatively small reduction in the length of the side chain (by one methylene group). This suggests that the length of the glutamine side chain is necessary for the carboxamide group to reach the interaction partner in the enzyme and/or to provide the conformational flexibility for it to fit into an occluded pocket. This is also consistent with our previous results that the diphosphorylated TDDEMpS-**Nle**-pYVAT (Nle = norleucine) (*11*) and Wip1(163pT) (EWPKpT**M**T-GLPS) (data not shown) peptides, which have the same side chain length but lack the carboxamide group, acted as poorer substrates than the corresponding peptides with glutamine at the +1 position. Likewise, the importance of the D264 residue of Wip1 for interaction with both classes of substrates is indicated by the fact that the D264A mutation resulted in reduced k_{cat}/K_m values for both the ATM(1981pS) and p38-(180pT 182pY) peptides (see the Results).

What appears evident now is that substrates of the two sequence motifs actually bind to the catalytic site of Wip1 in similar orientations and positions, as seen by comparison of the docked ATM and p38 peptide models (Figure 1A,B). The main difference is that the pSQ motif-containing substrates utilize the glutamine at the +1 position to form a secondary, stabilizing interaction and the pTXpY motif-containing substrates utilize the phosphotyrosine at the +2 position. First, that the binding sites are the same is indicated by the fact that the measured inhibition constant of the p38-derived, c(MpSIpYVAC) peptide was nearly the same when using either the native ATM (pSQ) or p38 (pTGpY) peptides as substrates. Further support comes from analyses of the effects of sequence changes in both the substrates and enzyme, including forming hybrid versions of the two sequence motifs. At the N-terminal of the bound substrates, similar positions for the negatively charged residues of the ATM and p38 peptides are indicated by similar effects due to charge-altering sequence changes (see Table 1 and ref *10*). For example, for the ATM substrate, double substitutions to nonpolar, Ala residues resulted in a 5-fold reduction in the k_{cat}/K_m value, while changes to positively charged Lys residues resulted in complete elimination of observable activity. According to the docking models (Figure 1A,B), these effects would be due to the progressive loss of electrostatic attraction and then repulsion with the conserved, positively charged R76 residue at the Wip1 active site. Likewise, at the C-terminal, similar bound positions for the two substrates are indicated by the similar effects of mutations at the +1 and +2 motif positions. As seen in Table 1 for the +2 position of the ATM substrate, substitution of the wild-type S1983 to negatively charged Asp, Glu, or phosphotyrosine residues (making the sequence more like that of the p38, pTXpY motif) all resulted in enhanced binding affinity and phosphatase activity, while the change to positively charged Lys resulted in significant loss of affinity. As previously demonstrated for the p38 substrate (*10*, *11*), that these negatively charged substitutions at the +2 position are interacting with the K238 of Wip1 is indicated in Figure 1C. Specifically, the K238D mutation in Wip1 resulted in the reverse effects of reduced activity for the ATM(S1983E) mutant peptide and enhanced activity for the ATM(S1983K) mutant. Likewise, that the +1 residues of the bound ATM and p38 peptides are also in the same location in the active site is indicated by a similar hybrid experiment shown in Table 2. In this case, changing the p38 pTGpY sequence to pTQpY, making it more like the ATM motif, resulted in an approximate 4-fold decrease in the K_m value, which indicates an increase in binding affinity. As described above, this is the same role revealed for the glutamine in the ATM pSQ motif shown in Table 1. Finally, that the Gln residue at the +1 position of both motifs is interacting with the D264 of Wip1 is indicated both by the docking simulations and by mutagenesis results. As seen in Figure 1A,B, having the pS/pT and the +2 residues anchored at the catalytically active position and the K238 residue, respectively, automatically positions the intervening +1 residue proximal to D264. This is also supported by previous studies showing that substituting a negatively charged residue at the +1 position of both the ATM(1893pS) (i.e., NLD-SEpS**E**HFFR) and p38 (i.e., TDDEMpS**D**pYVAT) substrates completely eliminated the catalytic activity (*8*, *11*), which would be due to the resultant electrostatic repulsion. A further experiment to test this hypothesis would be to try these two peptides with a D264K mutant of rWip1.

Additional information about the interacting residues in the bound complexes comes from comparing the kinetic results with those using the PP2Cα isoform. Similar to K238, which plays a large role in determining the selectivity of Wip1 for the p38-type substrates (*10*), the negatively charged D264 residue is unique to Wip1 among the PP2C family of phosphatases. That this determines the selectivity for the ATM-type substrates is supported by the fact that PP2Cα was unable to significantly dephosphorylate any of the p(S/T)Q-containing peptides tested as shown in Table 3. Furthermore, PP2Cα-catalyzed dephosphorylation of a p(S/T)Q-type substrate has not been reported in any other study of in vitro or in vivo phosphatase activity to date. While these

experimental results confirm the importance of the D264 and K238 residues in determining substrate selectivity, it is difficult to fully explain the physical basis in terms of the current homology model of Wip1. This, again, is because these residues are unique to the Wip1 isoform and do not have positions "confidently" defined by the PP2Cα crystal structure template (*18*). This is more of a problem for defining the location of D264, which is five residues from a template position, than the K238 residue, which is only two residues from a template position (*10*). Indeed, as we described previously (*11*), these residues are at the N- and C-terminal ends of a 25-residue loop unique to Wip1 that can easily fold over and contribute to the binding affinity of a substrate in the catalytic site. Thus, more accurate modeling of the reactions of Wip1 awaits additional structural information from X-ray crystallography and/or NMR analysis.

Inhibitors of Wip1. We previously demonstrated that the catalytic site of Wip1 is a good target for the development of specific inhibitors based on the p38(180pT 182pY) sequence (*11*). Using the p53(15pS) sequence, we synthesized an F_2Pab-substituted p53 peptide, Ac-VEPPLF_2-PabQpYTFS-NH_2, which inhibited rWip1 phosphatase activity with a K_i of 70 μM. This inhibitory activity indicated that not only the peptide with the pTXpY sequence but also a peptide with the p(S/T)Q sequence can interact with the catalytic site of Wip1 and inhibit its phosphatase activity. The K_i value of the Ac-VEPPLF_2PabQpYTFS-NH_2 peptide was weaker than that of the cyclic peptide c(MpSIpYVAC) previously reported (*11*). Thinking that the lower activity may be due to the conformational flexibility inherent with a linear peptide, we attempted to rigidify it by forming a cyclic analogue, i.e., c(LF_2PabQpYTYC). Unfortunately, unlike with the previous case (*11*), this approach did not lead to enhanced activity. To understand this result on a structural level, we determined the solution structure of the cyclic peptide c(LF_2PabQpYTYC) by NMR methods and modeled docking in the catalytic site of Wip1 (not shown). Consistent with the kinetic studies, it was found that, unlike the linear peptide (Figure 1A), the cyclic peptide cannot take advantage simultaneously of the three main sites of interaction. That is, for the specific rigid conformation of c(LF_2PabQpYTYC), having the two phosphate groups interacting with the metal center and K238 of Wip1 prevents the additional stabilizing interaction of the peptide's Gln with D264.

As described above, an additional factor that likely affects the binding affinity of both the linear and cyclic peptides is interaction with the 25-residue (239−263) loop near the catalytic site that is unique to the Wip1 isoform. We previously concluded (*11*) that the enhanced binding affinity of c(MpSIpYVAC) is likely due to a strongly specific, hydrophobic and steric interaction of the Ile residue and this "catalytic site loop". Needless to say, additional structural information of the conformation of this loop in the catalytic site of Wip1, by crystallography and/or NMR, would greatly help to optimize the activity of the c(LF_2PabQpYTYC) inhibitor by structure-based modeling approaches.

In conclusion, the results presented here and in our previous studies (*10*, *11*) firmly establish the unique substrate selectivity of Wip1 compared to the other members of the PP2C family and indicate some of the specific residue interactions responsible for this specificity. For example, it was demonstrated here that PP2Cα does not significantly catalyze the dephosphorylation of peptides with the ATM-type p(S/T)Q sequence motif and that the interaction with Wip1 is stabilized by interactions with the unique D264 and K238 residues. Thus, there is a great potential for developing highly selective, low molecular weight inhibitors of Wip1 suitable for in vivo biological testing and future drug development.

SUPPORTING INFORMATION AVAILABLE

Tables of kinetic parameters for the dephosphorylation of phosphopeptides by rWip1(K238D), rWip1(R110E), and rWip1(D264A). This material is available free of charge via the Internet at http://pubs.acs.org.

REFERENCES

1. Fiscella, M., Zhang, H., Fan, S., Sakaguchi, K., Shen, S., Mercer, W. E., Vande Woude, G. F., O'Connor, P. M., and Appella, E. (1997) Wip1, a novel human protein phosphatase that is induced in response to ionizing radiation in a p53-dependent manner, *Proc. Natl. Acad. Sci. U.S.A. 94*, 6048−6053.
2. Takekawa, M., Adachi, M., Nakahata, A., Nakayama, I., Itoh, F., Tsukuda, H., Taya, Y., and Imai, K. (2000) p53-inducible Wip1 phosphatase mediates a negative feedback regulation of p38 MAPK-p53 signaling in response to UV radiation, *EMBO J. 19*, 6517−6526.
3. Li, J., Yang, Y., Peng, Y., Austin, R. J., van Eyndhoven, W. G., Nguyen, K. C. Q., Gabriele, T., McCurrach, M. E., Marks, J. R., Hoey, T., Lowe, S. W., and Powers, S. (2002) Oncogenic properties of *PPM1D* located within a breast cancer amplification epicenter at 17q23, *Nat. Genet. 31*, 133−144.
4. Bulavin, D. V., Demidov, O. N., Saito, S., Kauraniemi, P., Phillips, C., Amundson, S. A., Ambrosino, C., Sauter, G., Nebreda, A. R., Anderson, C. W., Kallioniemi, A., Fornace, A. J., Jr., and Appella, E. (2002) Amplification of *PPM1D* in human tumors abrogates p53 tumor-suppressor activity, *Nat. Genet. 31*, 210−215.
5. Saito-Ohara, F., Imoto, I., Inoue, J., Hosoi, H., Nakagawara, A., Sugimoto, T., and Inazawa, J. (2003) PPM1D is a potential target for 17q gain in neuroblastoma, *Cancer Res. 63*, 1876−1883.
6. Hirasawa, A., Saito-Ohara, F., Inoue, J., Aoki, D., Susumu, N., Yokoyama, T., Nozawa, S., Inazawa, J., and Imoto, I. (2003) Association of 17q21−q24 gain in ovarian clear cell adenocarcinomas with poor prognosis and identification of *PPM1D* and *APPBP2* as likely amplification targets, *Clin. Cancer Res. 9*, 1995−2004.
7. Bulavin, D. V., Phillips, C., Nannenga, B., Timofeev, O., Donehower, L. A., Anderson, C. W., Appella, E., and Fornace, A. J., Jr. (2004) Inactivation of the Wip1 phosphatase inhibits mammary tumorigenesis through p38 MAPK-mediated activation of the $p16^{Ink4a}$-$p19^{Arf}$ pathway, *Nat. Genet. 36*, 343−350.
8. Shreeram, S., Hee, W. K., Demidov, O. N., Kek, C., Yamaguchi, H., Fornace, A. J., Jr., Anderson, C. W., Appella, E., and Bulavin, D. V. (2006) Regulation of ATM/p53-dependent suppression of myc-induced lymphomas by Wip1 phosphatase, *J. Exp. Med. 203*, 2793−2799.
9. Lu, X., Bocangel, D., Nannenga, B., Yamaguchi, H., Appella, E., and Donehower, L. A. (2004) The p53-induced oncogenic phosphatase PPM1D interacts with uracil DNA glycosylase and suppresses base excision repair, *Mol. Cell 15*, 621−634.
10. Yamaguchi, H., Minopoli, G., Demidov, O. N., Chatterjee, D. K., Anderson, C. W., Durell, S. R., and Appella, E. (2005) Substrate specificity of the human protein phosphatase 2Cδ, Wip1, *Biochemistry 44*, 5285−5294.
11. Yamaguchi, H., Durell, S. R., Feng, H., Bai, Y., Anderson, C. W., and Appella, E. (2006) Development of a substrate-based cyclic phosphopeptide inhibitor of protein phosphatase 2Cδ, Wip1, *Biochemistry 45*, 13193−13202.
12. Choi, J., Nannenga, B., Demidov, O. N., Bulavin, D. V., Cooney, A., Brayton, C., Zhang, Y., Mbawuike, I. N., Bradley, A., Appella, E., and Donehower, L. A. (2002) Mice deficient for the wild-type p53-induced phosphatase gene (*Wip1*) exhibit defects in reproductive organs, immune function, and cell cycle control, *Mol. Cell. Biol. 22*, 1094−1105.

13. Lu, X., Nannenga, B., and Donehower, L. A. (2005) PPM1D dephosphorylates Chk1 and p53 and abrogates cell cycle checkpoints, *Genes Dev. 19*, 1162−1174.
14. Shreeram, S., Demidov, O. N., Hee, W. K., Yamaguchi, H., Onishi, N., Kek, C., Timofeev, O. N., Dudgeon, C., Fornace, A. J., Anderson, C. W., Minami, Y., Appella, E., and Bulavin, D. V. (2006) Wip1 phosphatase modulates ATM-dependent signaling pathways, *Mol. Cell 23*, 757−764.
15. Fujimoto, H., Onishi, N., Kato, N., Takekawa, M., Xu, X. Z., Kosugi, A., Kondo, T., Imamura, M., Oishi, I., Yoda, A., and Minami, Y. (2006) Regulation of the antioncogenic Chk2 kinase by the oncogenic Wip1 phosphatase, *Cell Death Differ. 13*, 1170−1180
16. Oliva-Trastoy, M., Berthonaud, V., Chevalier, A., Ducrot, C., Marsolier-Kergoat, M. C., Mann, C., and Leteurtre, F. (2007) The Wip1 phosphatase (PPM1D) antagonizes activation of the Chk2 tumour suppressor kinase, *Oncogene 10*, 1449−1458.
17. Cheng, Y.-C., and Prusoff, W. H. (1973) Relationship between the inhibition constant (K_i) and the concentration of inhibitor which causes 50 per cent inhibition (I_{50}) of an enzymatic reaction, *Biochem. Pharmacol. 22*, 3099−3108.
18. Das, A. K., Helps, N. R., Cohen, P. T. W., and Barford, D. (1996) Crystal structure of the protein serine/threonine phosphatase 2C at 2.0 Å resolution, *EMBO J. 15*, 6798−6809.
19. Brooks, B. R., Bruccoleri, R. E., Olafson, B. D., States, D. J., Swaminathan, S., and Karplus, M. (1983) CHARMM: A program for macromolecular energy, minimization, and dynamics calculations, *J. Comput. Chem. 4*, 187−217.
20. Morris, G. M., Goodsell, D. S., Halliday, R. S., Huey, R., Hart, W. E., Belew, R. K., and Olson, A. J. (1998) Automated docking using a Lamarckian genetic algorithm and empirical binding free energy function, *J. Comput. Chem. 19*, 1639−1662.
21. Sanner, M. F. (1999) Python: a programming language for software integration and development, *J. Mol. Graphics Modell. 17*, 57−61.
22. Yaffe, M. B., Leparc. G. G., Lai, J., Obata, T., Volinia, S., and Cantley, L. C. (2001) A motif-based profile scanning approach for genome-wide prediction of signaling pathways, *Nat. Biotechnol. 19*, 348−353.
23. Freedman, D. A., Wu, L., and Levine, A. J. (1999) Functions of the MDM2 oncoprotein, *Cell. Mol. Life Sci. 55*, 96−107.
24. Michaelis, C., Ciosk, R., and Nasmyth, K. (1997) Cohesins: chromosomal proteins that prevent premature separation of sister chromatids, *Cell 91*, 35−45.
25. Shiloh Y. (2003) ATM and related protein kinases: safeguarding genome integrity, *Nat. Rev. Cancer 3*, 155−168.
26. Jackson, M. D., Fjeld, C. C., and Denu, J. M. (2003) Probing the function of conserved residues in the serine/threonine phosphatase PP2Cα, *Biochemistry 42*, 8513−8521.
27. Takekawa, M., Maeda, T., and Saito H. (1998) Protein phosphatase 2Cα inhibits the human stress-responsive p38 and JNK MAPK pathways, *EMBO J. 17*, 4744−4752.
28. Pinna, L. A., and Donella-Deana, A. (1994) Phosphorylated synthetic peptides as tools for studying protein phosphatases, *Biochem. Biophys. Acta 1222*, 415−431.
29. Chen, L., Wu, L., Otaka, A., Smyth, M. S., Roller, P. P., Burke, T. R., Jr., den Hertog, J., and Zhang Z. Y. (1995) Why is phosphonodifluoromethyl phenylalanine a more potent inhibitory moiety than phosphonomethyl phenylalanine toward protein-tyrosine phosphatases? *Biochem. Biophys. Res. Commun. 216*, 976−984.
30. Kim, S. T., Xu, B., and Kastan, M. B. (2002) Involvement of the cohesin protein, Smc1, in Atm-dependent and independent responses to DNA damage, *Genes Dev. 16*, 560−570.
31. Yazdi, P. T., Wang, Y., Zhao, S., Patel, N., Lee, E. Y., and Qin, J. (2002) SMC1 is a downstream effector in the ATM/NBS1 branch of the human S-phase checkpoint, *Genes Dev. 16*, 571−582.
32. Maya, R., Balass, M., Kim, S. T., Shkedy, D., Leal, J. F., Shifman, O., Moas. M., Buschmann T., Ronai, Z., Shiloh, Y., Kastan, M. B., Katzir, E., and Oren, M. (2001) ATM-dependent phosphorylation of Mdm2 on serine 395: role in p53 activation by DNA damage, *Genes Dev. 15*, 1067−1077.
33. O'Neill, T., Dwyer, A. J., Ziv, Y., Chan, D. W., Lees-Miller, S. P., Abraham, R. H., Lai, J. H., Hill, D., Shiloh, Y., Cantley, L. C., and Rathbun, G. A. (2000) Utilization of oriented peptide libraries to identify substrate motifs selected by ATM, *J. Biol. Chem. 275*, 22719−22727.
34. Abraham, R. T. (2004) PI 3-kinase related kinases: 'big' players in stress-induced signaling pathways, *DNA Repair 3*, 883−887.
35. Jackson, M. D., and Denu, J. M. (2001) Molecular reactions of protein phosphatases−insights from structure and chemistry, *Chem. Rev. 101*, 2313−2340.

BI701096S